J. Biochem. **140**, 175–184 (2006)
doi:10.1093/jb/mvj139

Structural Effects of a Covalent Linkage Between Antithrombin and Heparin: Covalent N-Terminus Attachment of Heparin Enhances the Maintenance of Antithrombin's Activated State

Tracy Anne Mewhort-Buist[1], Murray Junop[2], Leslie R. Berry[1], Paul Chindemi[2] and Anthony K. C. Chan[1,*]

[1]Department of Pediatrics, Henderson Research Centre, 711 Concession Street, Hamilton, ON, Canada L8V 1C3; and [2]Department of Biochemistry, McMaster University, 1280 Main Street West, Hamilton, ON, Canada L8S 4L8

Received February 3, 2006; accepted May 17, 2006

We have produced a molecule comprising of permanently-activated covalently linked antithrombin and heparin (ATH). This study was designed to elucidate the covalent linkage point(s) for heparin on antithrombin and conformational properties of the ATH molecule. ATH was produced using Schiff base/Amadori rearrangement by incubating antithrombin with unfractionated heparin for 14 d at 40°C. ATH was then digested using Proteinase K, and the heparin-peptide was reacted with $NaIO_4$/$NaBH_4$/mild acid to degrade the heparin moiety. Sequencing of the remaining peptide was performed by Edman degradation with linkage point confirmation by LC-MS. The degree of insertion of the reactive center loop (RCL) of antithrombin into the A-sheet of ATH was examined using synthesized antithrombin RCL peptides. Binding between the peptides and ATH, and the formation of ATH in the presence of the peptides were tested. CD was used to further examine the secondary and tertiary structures of ATH. The results suggest that heparin is conjugated to the amino terminal of antithrombin in the majority of ATH molecules, proximal to the previously determined heparin binding domain of antithrombin. From the linkage data, a model is proposed for the structure of ATH. Studies using the RCL peptides and CD analysis of ATH support this model.

Key words: antithrombin, coagulation factors, computer modeling, heparin, sequence.

Abbreviations: 2-ME, 2-β-mercaptoethanol; Tris HCl buffer, 0.05 M Tris HCl buffer pH 7.3; AT, antithrombin; ATH, antithrombin heparin covalent complex; RCL, reactive center loop; IIa, thrombin.

Heparin exerts its anticoagulant effects through its interaction with antithrombin (AT), leading to the inhibition of thrombin (IIa), a key player in the coagulation cascade. However, clinical use of heparin has many pitfalls, including, but not limited to, high variability in half-life, clearance (*1*), and dose-response (*2*) between patients, and the risk of heparin-induced thrombocytopenia (*3*). A covalently linked AT-heparin complex (ATH) has been developed in our laboratory (*4*). Previous studies have shown that ATH may overcome many of heparin's clinical disadvantages (*4–8*).

Chemical analysis of ATH has shown that it contains a keto-amine formed between a lysine ε-amino on AT and a sugar residue on heparin, confirming covalent linkage of the molecules (*9*). AT and heparin exist in a 1:1 molar ratio in ATH, and heparins containing the high affinity AT-binding pentasaccharide sequence are preferentially selected during the formation of ATH (*10*). A higher proportion of heparin molecules in ATH have multiple pentasaccharides compared to unfractionated heparin (*11*). Furthermore, the heparin moiety in ATH has an average molecular weight of 18,000, demonstrating that formation of ATH also selects for long chain heparins (*10*). Heparin chains on ATH have been shown to bind up to 1.5 molecules of exogenous AT (*11*), allowing catalysis of the reaction between exogenous AT and IIa.

AT exists in two isoforms, α and β (*12*), and there is a higher proportion of β-AT in ATH than in commercial AT (*13*). β-AT is more reactive to IIa than α-AT, however, in ATH, the difference between the two isoforms in the reaction with IIa is minimal (*13*). This result suggests a conformational difference between ATH and AT · heparin. The present study aimed to further elucidate the ATH structure by determining the linkage point on AT where heparin is covalently bound.

Crystal structures of AT have shown that it exists in a latent and an active state (*14*). In the latent state, the reactive center loop (RCL) of AT is fully inserted into the central β-sheet (A sheet), forming a six-stranded A sheet. In the active state, the RCL, up to P14 [Nomenclature adopted from Schechter and Berger, 1967 (*16–18*)], is inserted into the A sheet. Studies have shown that when AT is bound to high affinity heparin, exogenous RCL peptides corresponding to P1–P14 of the AT are not incorporated into the A sheet of AT (*15*). Thus, it has been suggested that that the RCL of AT may be inserted into the A sheet up to residues P12 or P10, when heparin is bound to AT (*14*). Since high affinity heparins are selected during ATH formation (*10*), and intrinsic fluorescence studies of ATH have shown that its AT is in a permanently

*To whom correspondence should be addressed. Phone: +1-905-527-2299 (Ext. 43559), Fax: +1-905-575-2646, E-mail: achan@thombosis.hhscr.org

activated state (*11*), the structure of ATH may allow for the RCL of AT to be partially inserted into the A sheet, similar to what occurs for AT·heparin. In this study, the degree of insertion of the RCL in ATH was examined by using peptides corresponding to P7–P14, P3–P14 and P1–P14 of the RCL of AT to compete with the RCL of ATH for insertion into the A sheet of ATH. Both far-UV and near-UV CD spectra were obtained to further examine the secondary and tertiary structures of ATH.

Finally, sequencing data for the heparin linkage point on ATH, and deductions about the conformation of ATH based on the RCL peptide interaction results and CD spectra were compared to published X-ray crystallographic structures of AT and AT·heparin to propose a model for the 3-dimensional tertiary structure of ATH.

EXPERIMENTAL PROCEDURES

Materials—All reagents were of analytical grade. AT was purchased from Affinity Biologicals (Hamilton, ON). Unfractionated heparin was purchased from Sigma Aldrich (sodium salt, grade I-A, from porcine intestinal mucosa. Mississauga, ON). RCL peptides were purchased from Quality Controlled Biochemicals Inc. (Hopkinton, MA). ^{3}H-$NaBH_4$ was obtained from Perkin Elmer (Woodbridge, ON). Protamine sulfate was from ICN (Irvine, CA).

ATH Preparation—The preparation of ATH has been described previously (*4*). Briefly, ATH was synthesized *via* Schiff base/Amadori rearrangement by incubating unfractionated heparin for 14 d with AT in a molar ratio of 200:1 in PBS, pH 7.3, at 40°C. Reduction of remaining Schiff base was achieved by adding $NaBH_3CN$ to the reaction mixture followed by incubation for an additional 5 h at 40°C.

ATH Purification—As previously described (*4*), ATH samples were purified in two steps. First, unreacted heparin was removed by hydrophobic chromatography using butyl-Sepharose. Second, unreacted AT was removed by anion exchange chromatography using a DEAE-Sepharose Fast Flow column.

Preparation of Heparin Linkage Peptides—ATH was dialyzed against 0.05 M Tris HCl buffer, pH 7.3, (Tris HCl buffer). Dialyzed ATH was then mixed with solid urea, Tris HCl buffer, and 2-β-mercaptoethanol (2-ME) to create a final concentration of 0.101 mM ATH in Tris HCl buffer containing 6 M urea and 0.005 M 2-ME. This solution was incubated for 1 h at 60°C. Tris HCl buffer, 1 M $CaCl_2$, and Proteinase K (Sigma) were added to the reaction mixture to achieve final concentrations of 0.033 mM ATH, 2.0 M urea, 0.005 M $CaCl_2$, 0.00167 M 2-ME, and 0.55 mg/ml Proteinase K. The reaction mixture was incubated for 20 h at 56°C. The reaction mixture was then purified by DEAE Sepharose anion exchange chromatography, to isolate only heparin-linked peptides, with 2-ME included in all buffer solutions. Bound heparin-peptide fragments were eluted using 2.0 M NaCl and 0.005 M 2-ME in 0.01 M Tris HCl buffer, pH 8.0. Free sulfhydryl groups were capped using 0.01 M iodoacetamide. Salts were removed by dialysis (12,000–14,000 Da cut off) against Milli-Q H_2O and then the samples were dried by lyophilization.

The heparin portion of the linkage peptide was cleaved using $NaIO_4$ and reduced with $NaBH_4$ following the method of Islam *et al.* (*19*). Lyophilized peptides were reconstituted in Milli-Q H_2O to give a theoretical heparin concentration of 10 mg/ml followed by incubation in 0.1 M $NaIO_4$, pH 5.0 for 20 h in the dark at 4°C with constant mixing. The peptide was dialyzed against Milli-Q H_2O and then reacted with 21.3 μl of 10 M NaOH for each ml of solution for 3.5 h in the dark at room temperature. Solid $NaBH_4$ was added to the reaction mixture to a final concentration of 0.02 M, followed by incubation for 4 h at room temperature. The pH of the solution was adjusted to 4.0 by drop-wise addition of 4 M HCl, with constant stirring. After 15 min the pH was adjusted to 7.0 with drop-wise addition of NaOH, followed by incubation at 4°C overnight. The purity of the linkage peptide was verified by SDS-PAGE. The peptide was dialyzed against Milli-Q H_2O using 100 Da molecular weight cut-off dialysis tubing and subsequently lyophilized.

Linkage Peptide Sequencing—The purified linkage peptide (1 mg) was reconstituted in 1 ml of 0.5% acetic acid, and then sent to Harvard Microchemistry (Harvard University, Cambridge, MA, USA) for amino acid sequencing involving Edman degradation, and peptide content determination by LC-MS analysis. Once completed, the sequences of the peptides prepared from the covalent heparin linkage site in ATH were compared with the known sequence for human AT (*20*) to deduce the amino acid linkage point(s) for heparin within ATH.

Peptide Preparation—Peptides corresponding to RCL residues P7–P14, P3–P14 and P1–P14 of human AT were capped and radiolabeled by reductive alkylation as described by Means and Feeney (*21*).

For radioactive labeling, 1.098 μmol of peptide were dissolved in H_2O to give a final concentration of 11.11 mg/ml. Borate buffer, pH 8.0 (0.2 M), was added to make a final concentration of 0.059 M borate, followed by the addition of 7.15 μl of 0.2 M H_2CO. The solutions were incubated for 20 min at room temperature. To each reaction mixture, 10 μl of 50 mCi/ml 0.2 M ^{3}H-$NaBH_4$ was added, followed by incubation for 2 h at room temperature. Next, 300 μl of 1 M HEPES buffer, pH 7.0, was added, before dialysis against 100 mM NaCl (100 Da cut-off). Radiolabeled peptides were stored at 4°C.

For non-radioactive capping, peptides were dissolved in H_2O to give a concentration of 11.11 mg/ml. Next 0.38 ml of 0.2 M borate, buffer pH 8.0, was added to 0.9 ml of each peptide solution, followed by the addition of 0.045 ml of 0.2 M H_2CO. The reaction mixtures were incubated at room temperature for 20 min. The addition of 0.05 ml of 0.2 M $NaBH_4$ was followed by further 2 h incubation at room temperature. Next, 0.25 ml of 1 M HEPES, pH 7.0, was added to each sample prior to dialysis against 0.1 M NaCl (100 Da cut-off). The peptides were lyophilized and stored at room temperature. Peptides were reconstituted in 0.02 M phosphate buffer, pH 7.3, and then stored at 4°C.

Binding of RCL Peptides to AT or ATH—Varying concentrations of radiolabeled peptides (0–3.0 μM) were incubated with 1.0 μM AT ± 3.0 μM unfractionated heparin or with 1.0 μM ATH in Tris HCl buffer at 37°C (total sample volume = 1.1 ml). Samples were dialyzed (12,000–14,000 Da cut-off) against 9 ml Tris HCl buffer for 24 h at 37°C, with constant rotation on an automated

rotator (Glas-Col, Terre Haute, IN). Following dialysis, the volumes of the solutions inside and outside the dialysis tubing were measured. The amount of peptide bound to AT or ATH was quantified by measuring the radioactivity in samples taken from inside and outside the dialysis tubing. Samples were added (0.5 ml) to 0.5 ml of Milli-Q H2O and 9 ml of BCS Scintillant (Amersham Biosciences Inc., Baie d'Urfé, QC) in glass scintillation vials, and counted using an LS 6000LL β-counter (Beckman, Fullerton, CA). The 0 mM samples were used as blanks. Since supersaturated stock solutions of P3–14 and P1–P14 were prepared, the samples were centrifuged, and a portion of the supernatant was taken for each experiment. In order to ensure the concentration of the supernatant was consistent, reference samples were measured each day, and compared to CPM values for the starting supernatants (*i.e.*, upon first preparation of the peptide) to determine the concentrations of the peptides. The concentrations of the samples were corrected by multiplying them by the ratio of the reference sample CPM value and the starting CPM value. The results were expressed as bound *vs.* free peptide in moles.

ATH Preparation in the Presence of Peptides—ATH was prepared, as described above, by incubating AT with unfractionated heparin in the presence of each of the reductively alkylated RCL peptides: P7–P14, P3–P14, and P1–P14, in a molar ratio of H:AT of 54:1. The reaction volume was 2 ml containing 16.9 μM AT, 926 μM unfractionated heparin, and 1.0 μM peptide in PBS. Reagents were added in the following order: PBS, peptide, heparin concentrate in PBS, and AT concentrate in PBS, with mixing before the addition of AT. Purification of the ATH formed followed the procedure described above. Remaining RCL peptides were removed by dialysis between the two chromatographic purifications (12,000–14,000 Da cut-off). The concentrations of ATH, expressed in mg/ml, were determined by measuring the A_{280} on a SpectraMax Plus 384 spectrophotometer (Molecular Devices, Sunnyvale, CA), and dividing it by the previously determined extinction coefficient for ATH of 0.75 $A_{280} \cdot mg^{-1} \cdot ml$ (*6*). ATH samples were stored at 4°C until analysis of heparin anti-Xa activity.

Anti-Xa Activity of ATH Samples—Samples were diluted in bovine serum albumin to a concentration of 0.03 μg/ml (in terms of AT), and then sent to the Hemostasis Reference Laboratory (Hamilton, ON) to assess heparin activity. Heparin anti-Xa activity was measured using a Stachrom heparin colorimetric assay and an unfractionated heparin standard curve (Diagnostica Stago, Ansières, France). The absorbance at 405 nm was measured using an Amax 190+ spectrophotometer (Trinity Biotech, Bray, Ireland). The remaining undiluted sample was stored at –80°C.

Protamine Sulfate Assay of Heparin—Use of the protamine sulfate assay for quantifying heparin has been previously reported and verified (*10*, *22*). In brief, 0.1–0.2 ml of each ATH sample was diluted in H_2O to a final volume of 0.5 ml. Subsequently, 0.2 ml of 1 mg/ml protamine sulfate was added to each sample, with immediate vortexing. The timing of the addition of the protamine sulfate was equally spaced at 10 s between samples. After 10 minute incubation, 1 ml of 0.1 M L-arginine · HCl was added to each sample, with immediate vortexing, to stop the protamine reaction. The addition of L-arginine · HCL was equally spaced at 10s between samples. The samples were then diluted with 1 ml of 0.1 M Tris HCl, pH 8.0. From each sample, 0.2 ml was removed and placed in a 96-well plate. Samples were read on a SpectraMax Plus 384 spectrophotometer (Molecular Devices, Sunnyvale, CA), and the A_{470} for each sample was compared to a standard curve of stock reference ATH to determine the concentration of heparin in each sample. The molar ratio of antithrombin to heparin in each ATH sample was calculated using these data.

CD Analysis—CD spectra were obtained using a Jasco J-600 spectropolarimeter. For far-UV spectra, 0.450–0.225 mg/ml samples of AT, AT · heparin, and ATH (concentrations in terms of mg AT) were scanned from 250 nm to 190 nm at 23, 37, 40, 45, and 50 ± 1°C. Heparin was in a 1:1 ratio with AT in AT · heparin. The temperature was maintained using a MGW Lauda RC6 water bath (Brinkmann, Westbury, NY, USA) attached to a 0.1 cm jacketed optical cuvette. Spectra were the means of 10 accumulations acquired at 100 nm/minute, with 50 mdeg sensitivity and a 0.5 s time constant. Baselines were obtained by scanning either PBS or 0.114 mg/ml heparin for AT and AT · heparin or ATH, respectively. The mean residue molar ellipticity was calculated by dividing the molar ellipticity by the number of peptide bonds in AT, and expressed in units of $deg \cdot cm^2 \cdot dmol^{-1}$.

For near-UV spectra, 1.475 mg/ml samples of AT, AT · heparin, and ATH (concentrations in terms of mg AT) were scanned from 320 nm to 250 nm. Heparin was in a 7:1 ratio with AT in AT · heparin. AT · heparin was scanned at 23, 37 and 40 ± 1°C. Since there were no significant differences in the spectra, subsequent samples were scanned at 23 and 40 ± 1°C only. A 1 cm jacketed optical cuvette was used. Spectra were the means of 10 accumulations acquired at 20 nm/min, with 10 mdeg sensitivity and a 2.0 s time constant. Baselines were obtained by scanning either PBS or 2.625 mg/ml heparin. The mean molar ellipticity was calculated and expressed in units of $deg \cdot cm^2 \cdot dmol^{-1}$.

Model Building—A model was constructed to explain data generated in the present linkage studies of AT and heparin in ATH based on the reported crystal structure of AT bound to the heparin pentasaccharide and thrombin [PDB 1TB6, (*2*)]. A model for a polysaccharide substrate containing two sugar moieties at the –1 and –2 positions of the heparin pentasaccharide was first built using program O (*23*). Appropriate constraints for both geometries and torsion angles of this molecule were then generated using program XPLO2D (*24*). Program O (*23*) was used for further model building, which was required to position amino acid residues 1–8 of AT and the terminal saccharides of heparin such that the His1 primary amine was close enough to C1 on the –2 saccharide of heparin for chemical cross-linking. Amino acid residues 1–8 of AT were modeled as an extended loop.

Statistical Analysis—General linear ANOVAs were performed to examine differences between groups. Where differences were found, two sample *t*-tests for independent groups were used to clarify group differences. All statistics were performed using Minitab. A value of $p < 0.05$ was considered significant. The results are expressed as mean ± SEM.

RESULTS

Heparin Linkage Peptide Sequencing—The AT polypeptide in ATH was cleaved using Proteinase K, followed by purification of the heparin-containing peptides (heparin linkage peptides) on a DEAE-Sepharose anion exchange chromatography column. The heparin moiety was digested using periodate oxidation, followed by borohydride reduction and mild acid hydrolysis. Amino acid sequence analysis by Harvard Microchemistry yielded two potential sequences for peptides recovered in the preparation. A covalent linkage through Schiff base/Amadori rearrangement requires an amino group to react with a carbohydrate aldose moiety. Therefore, the linkage point can only exist at the amino terminus of AT or at an ε-amino of a Lys residue. Further separation and sequence analysis of peptides by LC-MS (Harvard Microchemistry) revealed a population of fragments derived from the sequence His-Gly-Ser-Pro-Val, a sequence uniquely expressed at the N-terminus of AT (*20*). Small CHO fragment groups attached to the N-terminal His residue were observed in the LC-MS scans, which were likely remnants of the degraded heparin chain. In addition to the N-terminal linkage point, Edman degradation analysis indicated that a minority of heparin in the digest was linked to a peptide with a unique Ser-Ser sequence that occurs near the reported heparin-binding domain of AT, close to the Asn135 glycosylation site (*20*). Directly adjacent to the Ser-Ser sequence in AT is Lys139, the putative heparin linkage point. Thus, two points of covalent attachment for heparin to AT were identified. The relative occurrence of linkage of heparin to the N-terminal amino acid and Lys139 was 87% and 13%, respectively.

Binding of RCL Peptides to AT or ATH—Binding between the RCL peptides and either AT (in the presence or absence of heparin) or ATH was examined by incubating radiolabeled peptide with AT or ATH, and measuring free and bound peptide after equilibrium dialysis. No binding to AT in the presence or absence of heparin, nor to ATH was seen using the P7–P14 peptide (data not shown). The aqueous solubility of the P3–P14 and P1–P14 peptides limited the concentration range that could be studied. At an α level of 0.05, significant binding was observed between the P3–P14 peptide and AT, AT · heparin, and ATH (Fig. 1). Binding to ATH and AT · heparin was significantly higher than that to AT alone when 1.0×10^{-9} mol of P3–P14 were used. There was a trend towards increased binding with AT · heparin compared to binding of AT alone or ATH, but it did not reach statistical significance. Significant binding to AT was observed, but not to AT · heparin or ATH in the P1–P14 condition (Fig. 2). Furthermore, binding between P1–P14 and AT was much lower than that observed between P3–P14 and AT, with maximum bound peptide at 7.58×10^{-12} mol and 6.44×10^{-11} mol, respectively.

ATH Preparation in the Presence of Peptides—ATH was prepared using the standard conditions and purification protocol (*4*), except that the H:AT molar ratio was 54:1, and that the RCL peptides were added to the reaction mixtures. There was no statistically significant difference in the percent recovery, anti-Xa activity, or AT:heparin ratio between the different ATH preparation conditions (Fig. 3). However, a slight trend towards reduction in ATH formation may have occurred with the P7–P14 and P3–P14 peptides, which represent portions of the RCL more distal to the reactive

CD Analysis—There was no significant effect of temperature on the far-UV CD spectra of AT (data not shown), AT · heparin (Fig. 4A), or ATH (data not shown). The spectra of AT and AT · heparin, were super-imposable, while the ATH spectrum was slightly elevated at 40°C (Fig. 4B). The error bars, representing the SEM of the data, overlapped considerably (omitted for clarity), indicating that this difference was not statistically significant.

Similarly, there was no significant effect of temperature on the near-UV CD spectra of AT, AT · heparin, or ATH (Fig. 4C). However, the addition of heparin caused an increase in the ellipticity of AT, consistent with previous findings (*25–27*). Covalent linkage of the heparin to AT caused a further increase in the curve within the 290 to 250 nm range of the spectrum, accompanied by a change in the relative strength of the four peaks in this region.

Molecular Model Construction—Based on results of the linkage studies on AT and heparin, a model of ATH was constructed (Fig. 5). This model is based on the ATH linkage site data, and is consistent with the RCL and CD data.

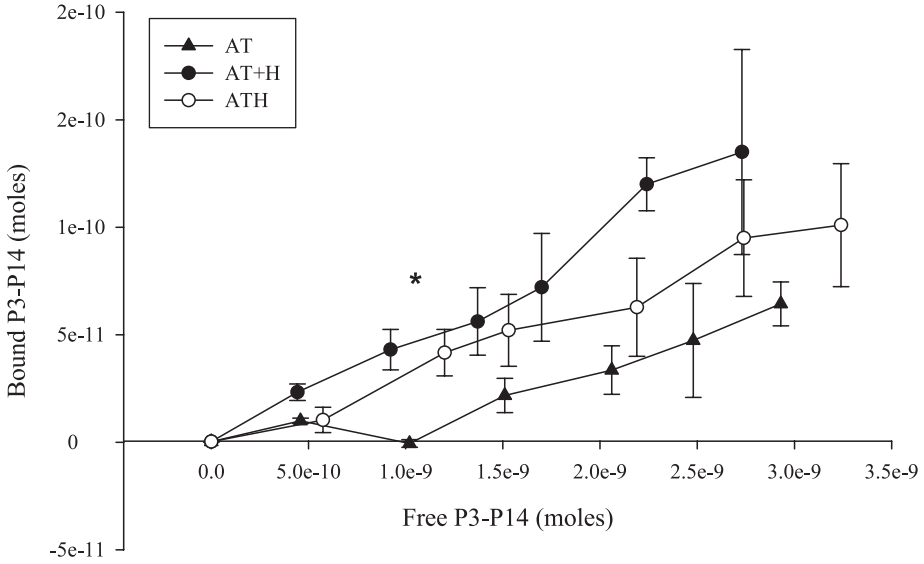

Fig. 1. **Binding of P3–P14 to antithrombin (AT), AT + heparin (H), and antithrombin-heparin covalent complex (ATH).** Radiolabeled P3–P14 was incubated with 1 μM AT, 1 μM AT + 3 μM H, or 1 μM ATH, and equilibrium dialysis was carried out for 24 h at 37°C. The amount bound was calculated by scintillation β-counting of the solutions inside and outside the dialysis tubing. Data points represent the means of 2–4 experiments ± SEM. Significance between data sets was determined using ANOVA. Where significance was found, results were further analyzed using 2-sample Student's *t*-tests. * Both AT+H and ATH exhibited greater P3–P14 binding than did AT, $p < 0.05$.

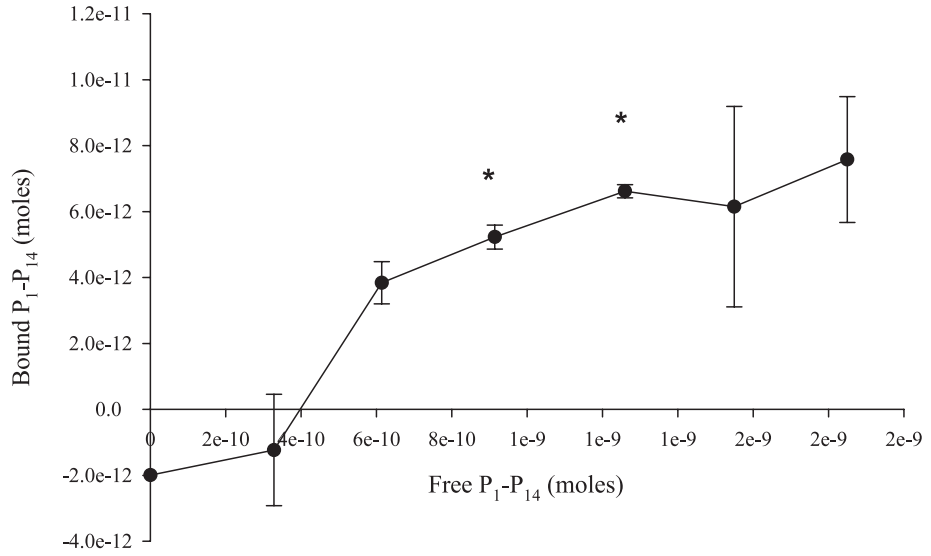

Fig. 2. **Binding of P1–P14 to antithrombin (AT).** Radiolabeled P1–P14 was incubated with 1 μM AT and equilibrium dialysis was performed for 24 h at 37°C. The amount bound was calculated by scintillation β-counting of the solutions inside and outside the dialysis tubing. Data points represent the means of two experiments ± SEM. Significance was determined by a 1-sample Student's *t*-test. * = $p < 0.05$.

Since RCL peptide-binding and CD spectra indicated that much of the ATH conformational characteristics were similar to those of non-covalent AT·heparin, the model was based on the previously determined crystal structure of AT bound to the heparin pentasaccharide and thrombin [PDB 1TB6, (*2*)]. ATH model building was performed with all amino acid side chains present and there were no resulting steric clashes within any portion of the ATH model (see "EXPERIMENTAL PROCEDURES"). The predominant cross-linked species reported here results from the interaction of the free aldose of heparin and the primary amine present at the N-terminus of AT, found to represent the linkage point in 87% of all ATH molecules. As shown in Fig. 5A, when residues 1–8 of AT are in an extended conformation, the primary amine of His1 can be positioned within covalent linking distance of heparin. Although no alteration in the core pentasaccharide itself or the pentasaccharide binding region of AT was required to produce the final ATH model, the pentasaccharide on its own was not sufficiently long to permit this interaction. As shown in the model of ATH, two additional sugar moieties are required at the –1 and –2 positions of the pentasaccharide sequence to bring the terminal aldose C1 within bonding distance of the His1 α-amino. Figure 5B displays most of the ATH structure, with the heparin chain shown as it extends away from the pentasaccharide binding site and linkage region. In magenta is the second putative heparin linkage domain in ATH, Lys139. As is clear from the model, several additional saccharides would be required at the pentasaccharide end of heparin for the pentasaccharide to be in the binding domain of AT in ATH molecules linked at this residue. As seen in Fig. 5C, the proposed structure of ATH does not interfere with the proposed interaction between AT, heparin, and IIa (*2*).

DISCUSSION

The covalent molecule comprising heparin and AT that has been produced in our laboratory overcomes most clinical problems of heparin, while maintaining its benefits in anticoagulation (*4–8*). Previous work by our laboratory has shown that AT and heparin in ATH exist in a 1:1 ratio (*4*), and that there is a higher proportion of β-AT in ATH than in the starting plasma AT (*13*). Studies examining the heparin moiety of ATH have shown that all heparin chains in ATH contain a pentasaccharide sequence, with at least 30% of all chains containing two pentasaccharides. This study further characterized the structure of ATH.

The sequencing data obtained in this study suggest that the majority of ATH has heparin linked at the α-amino group on the N-terminal amino acid His1, with a small population of molecules exhibiting covalent heparin linkage to the ε-amino group of Lys139, both of which are near the putative heparin-binding domain of AT (*20*). While linkage to Lys139 confirms the covalent keto-amine linkage structure between an AT Lys ε-amino and heparin uronic acid residue described previously (*9*), heparin conjugation at the His1 α-amino is a novel finding. Although separated by many residues in the primary structure, His1 and Lys139 are in close proximity within the tertiary structure of AT (*2*). Residues 24, 47, 125, 129, 132, and 133 have been regarded as being critical for heparin-binding to AT (*28*, *29*), with the 47 and 129 ones being essential for pentasaccharide binding (*29*). These data are consistent with the ATH heparin linkage point being associated with the pentasaccharide binding region on AT, as suggested previously (*4*).

It has been previously demonstrated that ATH consists of 45% β-AT and 55% α-AT (*13*). The key difference between these isoforms is the lack of a glycan at Asn135 in β-AT. Glycosylation of Asn135 could lead to steric hindrance of ATH formation at Lys139. Thus, all Lys139-linked ATH is likely composed of β-AT. In contrast, His1-linked ATH may occur with both isoforms, which likely explains its prevalence over the Lys139-linked ATH.

Binding studies using the RCL peptides suggested that the binding of heparin causes a conformational change in AT which prevents insertion of the RCL peptide into the molecule. Chang *et al.* (*30*) showed 70% binary complex formation between AT and P3–P14 using a 5:1 peptide:AT ratio. This is a much higher level of binding compared to our results, possibly due to differences in procedure. Increased binding of P3–P14 to AT in the presence of

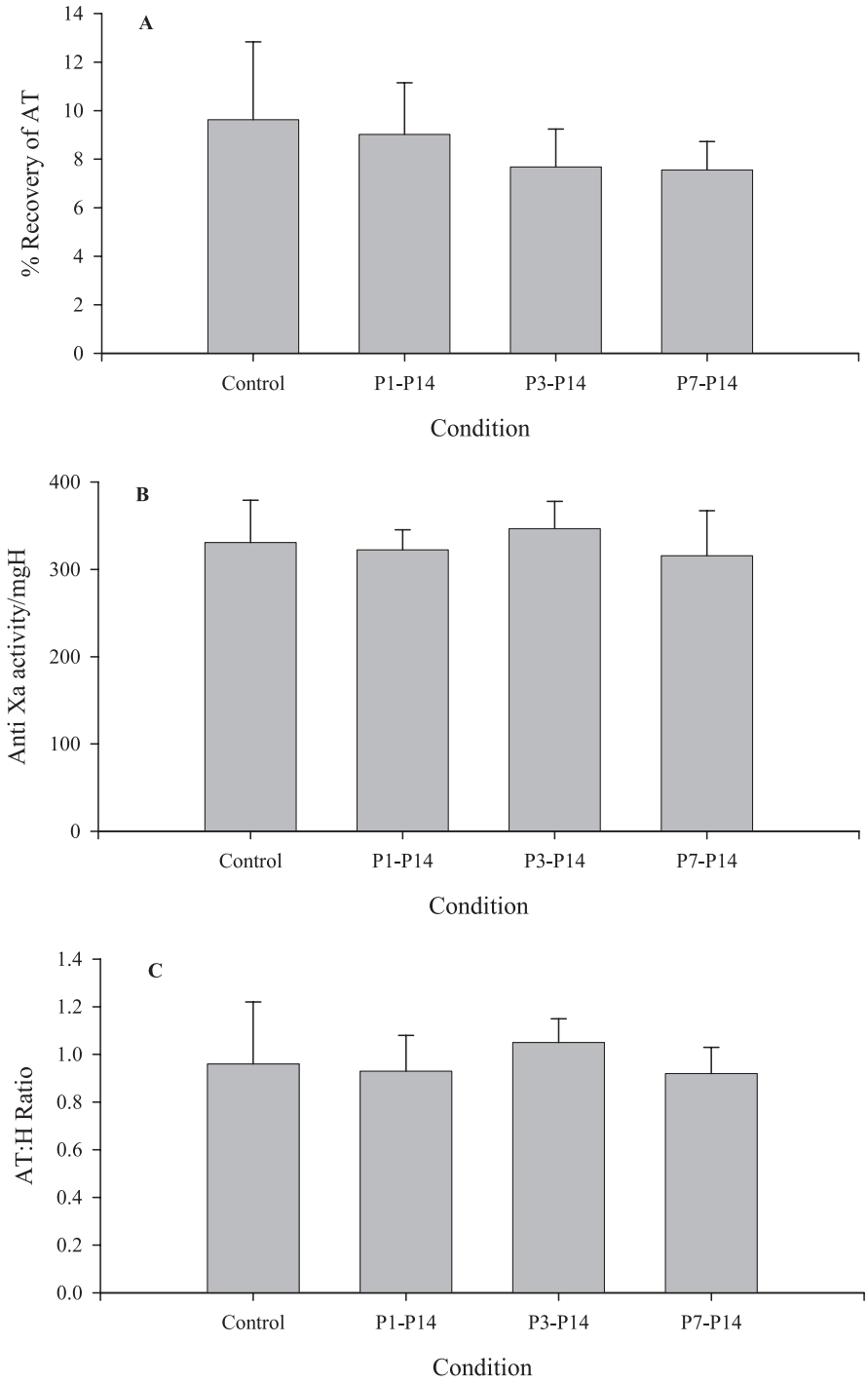

Fig. 3. **Formation of antithrombin-heparin covalent complex (ATH) in the presence of antithrombin (AT) reactive centre loop (RCL) peptides.** Peptides corresponding to the P7–P14, P3–P14 and P1–14 residues of the RCL of AT (1 μM) were incubated with 16.9 μM AT and 926 μM heparin (H) in PBS at 40°C for 14 days. The results are the means for 5–6 samples ± SEM. Panel A shows the percent recovery of AT. The AT content was measured by determining the A_{280} of the samples, and dividing it by the extinction coefficient for ATH of 0.75 $A_{280} \cdot mg^{-1} \cdot ml$. Panel B shows the anti-Xa activity of the ATH samples expressed in units/mg of heparin, as measured by a commercially-available colourimetric assay (Diagnostica Stago, Ansières, France). Panel C gives the AT:H ratios of purified ATH samples. The heparin content was measured using a protamine sulfate assay, and compared to the AT content, measured spectrophotometrically.

heparin compared to P1–P14 may infer that the conformational change affects the insertion of the P1–P2 region of the peptide. Pike *et al.* (*31*) have suggested that P1 Arg is bound to the body of AT during initial heparin binding, distorting the RCL, which was later supported by Owen *et al.* (*28*). If a similar conformation exists in ATH, this binding may prevent P1–P14 from being inserted into the A sheet. These data are consistent with the AT in ATH being in a partially inserted, activated conformation, similar to what has been previously seen with non-covalent AT · heparin. Our data for P1–P14 are also consistent with previous studies that have shown that stable complex formation between the peptide and AT was greatly reduced in the presence of high affinity heparin (*15*).

The formation of ATH was not significantly affected by the presence of the RCL peptides in the reaction mixture. Pentasaccharide-mediated binding of heparin to AT exhibits a very high dissociation rate (*32*), and previous studies in our laboratory have shown that ATH formation does not begin until the sixth day of incubation (*9*). In contrast, complexes between AT and P1–P14 or P3–P14 occur within 24 h (*15*). The results may suggest that interaction of the

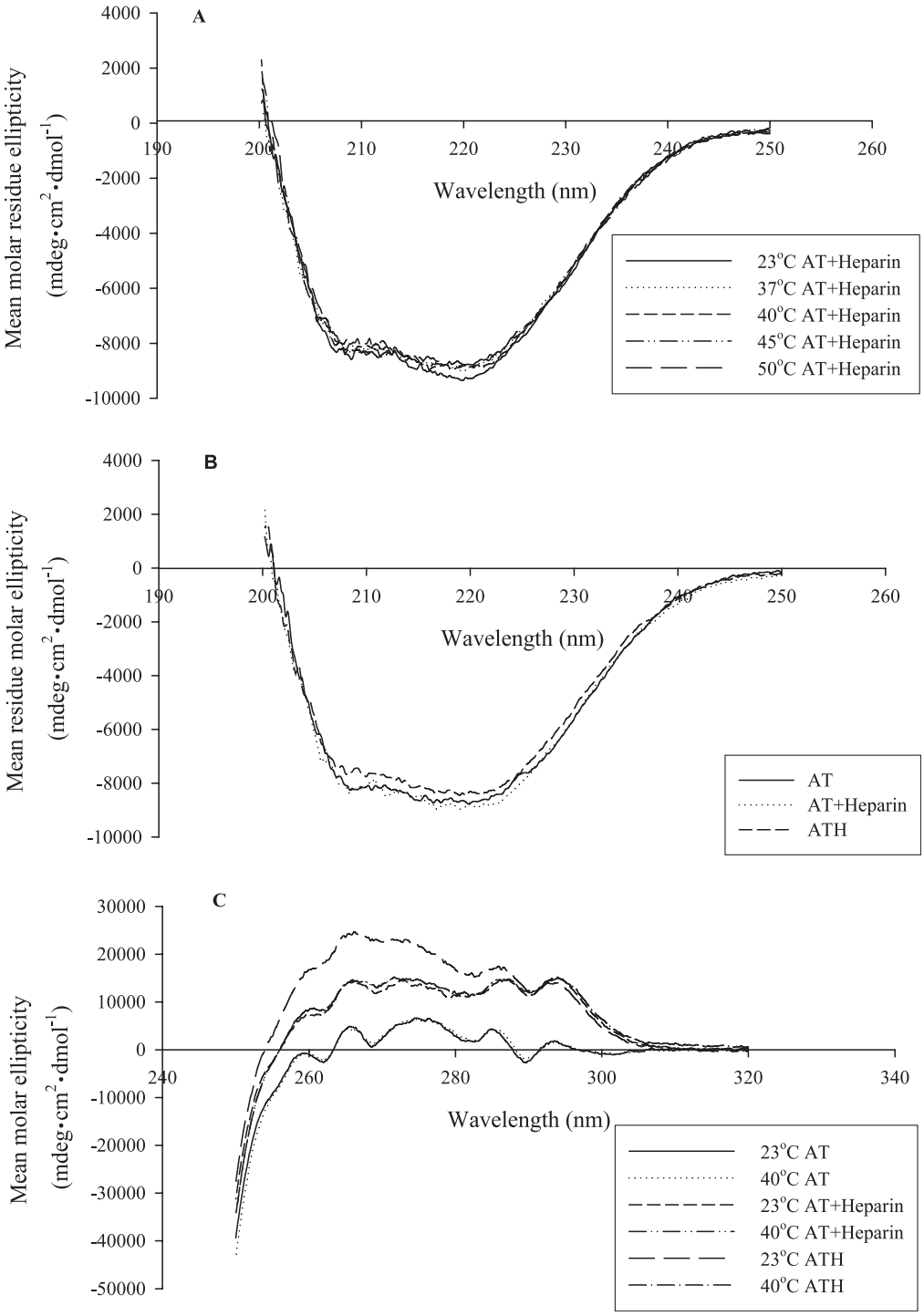

Fig. 4. **Circular dichroism spectra of antithrombin (AT), AT+heparin, and antithrombin-heparin covalent complex (ATH) at varying temperatures.** Data are means for two experiments, with 10 accumulations for each experiment. The PBS baseline was subtracted from AT spectra, while the heparin baseline was subtracted from AT+heparin and ATH spectra. Panel A shows the far-UV spectra of AT+heparin at 23, 37, 40, 45, and 50 ± 1°C. Panel B shows the far-UV spectra of AT, AT+heparin and ATH at 40 ± 1°C. Panel C shows the near-UV spectra of AT, AT+heparin, and ATH at 23 and 40 ± 1°C.

peptide with AT does not likely alter the AT conformation sufficiently to preclude proper orientation of the molecule for covalent attachment of heparin at the aldose terminus. Alternatively, heparin may have the ability to displace the reactive centre loop peptides from the A sheet. Other studies are warranted to examine these possibilities.

There were no significant differences in the far-UV or near-UV CD spectra as a result of temperature, demonstrating that there is no large structural change in AT on heating. Thus, the thermally-induced increase in the ATH yield (*4*, *9*) cannot be explained by this mechanism. Similarly, there were no significant differences in the far-UV spectra of AT, AT·heparin, and ATH. However, a difference was seen in the near-UV spectra of ATH compared to AT·heparin, suggesting changes in tertiary structure upon covalent linkage of heparin. Increases in molar ellipticity usually reflect the movement of Trp, Phe and Tyr residues towards the interior globule core of the protein, and an increase in protein rigidity. These changes should be clarified further.

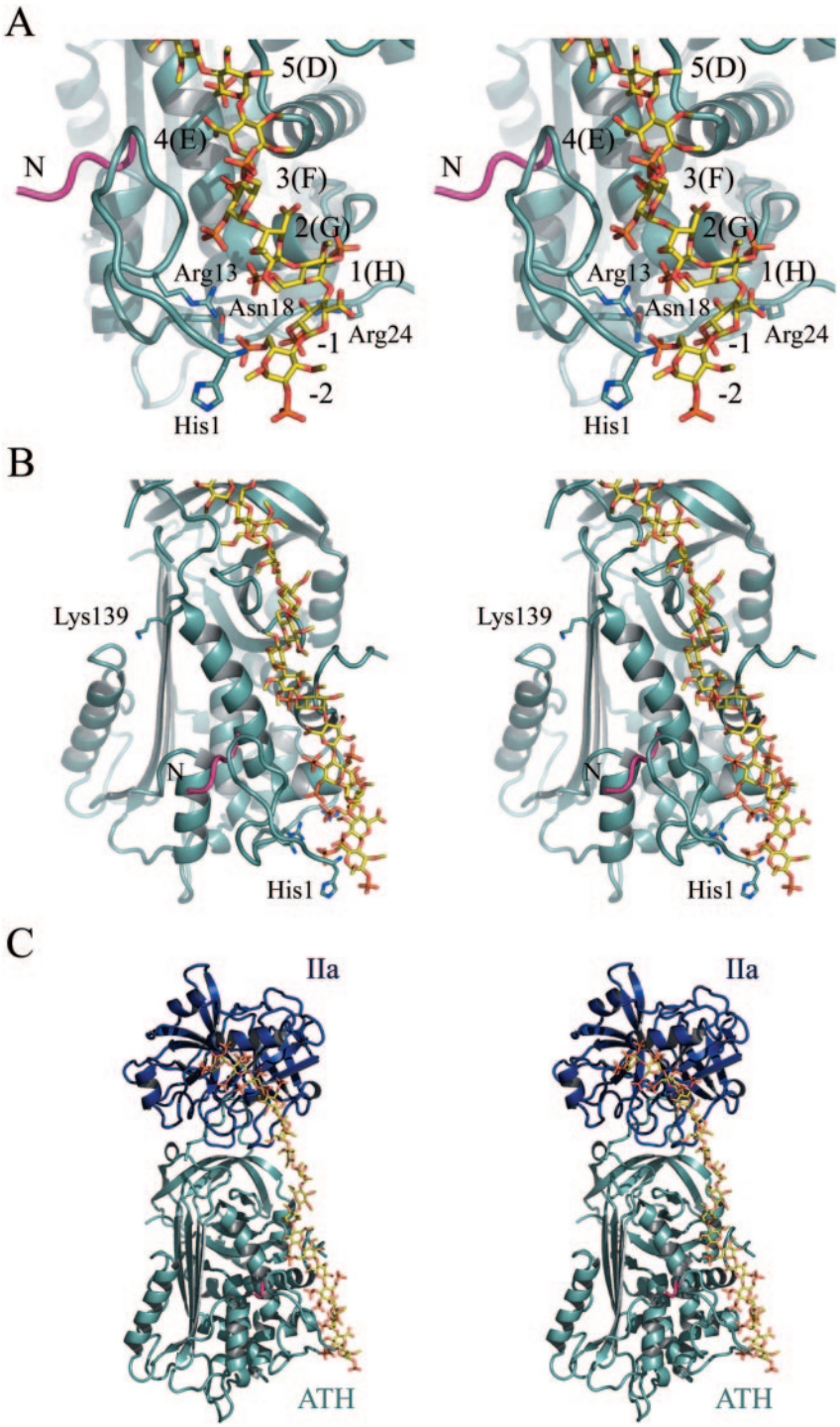

Fig. 5. **Antithrombin-heparin covalent complex (ATH) structural model.** Panel A shows a comparison of the N-terminal regions of antithrombin (AT) and ATH. ATH is represented by a light blue ribbon. The N-terminal residues of AT which become reordered upon ATH formation are indicated in magenta. The residues of AT predicted to interact with heparin (H) are shown in stick form. Panel B illustrates the relative position of Lys139 within the heparin binding cleft of AT. Panel C is a model of the ternary complex of thrombin (IIa) with AT and heparin of ATH.

Since the peptide and CD studies suggested that the protein conformation in ATH closely resembles that in non-covalent AT·heparin it seemed valid to develop a structure for the major ATH linkage species using AT·pentasaccharide X-ray data (*2*). Although alternative ATH models involving entirely uncharacterized AT·pentasaccharide binding could account for the observed interaction of His1 and heparin, the one presented in Fig. 5 is consistent with the current knowledge of structural requirements necessary for productive binding between AT and heparin. A heparin aldose linkage to the AT N-terminus would require full extension of amino acids 1–7 (Fig. 5). In all previous structures of AT, the N-terminal residues (~4) are either entirely disordered or highly mobile, as reflected by B values of typically greater than 60 $Å^2$. Presumably this apparent lack of structure at the N-terminus of AT reflects the ability of these residues to adopt many conformations. Similarly, the linkage requires the extension of the pentasaccharide by at least two saccharides. This agrees with

fluorophore-assisted carbohydrate electrophoresis data demonstrating that the shortest heparin chains recovered from ATH preparations are seven saccharide units long (*10*). Even with torsion angles adjusted optimally so that these two sugar residues extend back toward the His1 position of AT, there is just sufficient distance from heparin and the mobile N-terminal residues of AT to accommodate the link proposed in the current ATH model. Consequently, this model predicts a steric barrier along the path toward a productive interaction of reactive heparin aldose and primary amine. This barrier may at least partly account for the elevated temperature (≥40°C) conditions preferred for production of ATH (*4*, *9*).

Despite the presence of several potentially reactive primary amine groups among lysine residues on the surface of AT, sequence analysis revealed that only a minority of ATH molecules are linked at a single lysine residue at position 139. Figure 5B illustrates the position of Lys139 within AT, which is located over 20 Å away from the reactive aldose at the –2 position of heparin. When heparin is bound to AT *via* a high-affinity pentasaccharide group, its reactive aldose group is too far from Lys139 to permit interaction. Thus, it would seem most probable that this highly exposed Lys residue is attached to heparin in a pentasaccharide-independent manner. This type of structure may coincide with the small fraction of ATH molecules (12%) that exhibit low (or no) binding affinity to immobilized AT (*10*). Determination of whether this linkage is non-specific or occurs in an alternative heparin-binding dependent manner requires further study.

Two additional pieces of evidence favor our current ATH structural model. First, there are two Cys disulfide bridges at positions 8 and 21, which prevent further unraveling of the N-terminus of AT. It could be argued that further disorder at the N-terminus would be necessary or beneficial to accommodate the N-terminal linkage, yet, this is not possible. Second, it could be suggested that the elevated temperature used to yield ATH causes sufficient unfolding in the pentasaccharide binding cleft of AT to permit a different mode of AT · heparin interaction that may account for the covalent bonding to His1 or Lys139. Yet, far-UV CD studies (Fig. 4, A and B) did not show temperature-dependent secondary structure changes supporting such an argument.

With the present studies, essentially all primary, and much of the tertiary, structural analyses of ATH are complete. X-ray crystallography of ATH is one of the final steps required to confirm the structural models of this novel compound.

Dr. Vettai S. Ananthanarayan is gratefully acknowledged for discussion of the CD spectropolarimetric data. Helen Atkinson, Kevin Cheung, Aaron Kerman, and Lesley Smith are acknowledged for their technical assistance. This work was supported by a Grant-in-Aid (T5414) from the Heart and Stroke Foundation of Ontario. Anthony Chan is a Career Investigator of the Heart and Stroke Foundation of Canada.

REFERENCES

1. Hirsh, J., van Aken, W.G., Gallus, A.S., Dollery, C.T., Cade, J.F., and Yung, W.L. (1975) Heparin kinetics in venous thrombosis and pulmonary embolism. *Circulation* **53**, 691–695
2. Li, W., Johnson, D.J.D., Esmon, C.T., and Huntington, J.A. (2004) Structure of the antithrombin-thrombin-heparin ternary complex reveals the antithrombotic mechanism of heparin. *Nat. Struct. Mol. Biol.* **11**, 857–862
3. Warkentin, T.E., Levine, M.N., Hirsh, J., Horsewood, P., Roberts, R.S., Gent, M., and Kelton, J.G. (1995) Heparin-induced thrombocytopenia in patients treated with low-molecular-weight heparin or unfractionated heparin. *N. Engl. J. Med.* **332**, 1330–1335
4. Chan, A., Berry, L., O'Brodovich, H., Klement, P., Mitchell, L., Baranowski, B., Monagle, P., and Andrew, M. (1997) Covalent antithrombin-heparin complexes with high anticoagulant activity: Intravenous, subcutaneous and intratracheal administration. *J. Biol. Chem.* **272**, 22111–22117
5. Chan, A.K.C., Paredes, N., Thong, B., Chindemi, P., Paes, B., Berry, L.R., and Monagle, P. (2004) Binding of heparin to plasma proteins and endothelial surfaces is inhibited by covalent linkage to antithrombin. *Thromb. Haemost.* **91**, 1009–1018
6. Berry, L.R., Becker, D.L., and Chan, A.K.C. (2002) Inhibition of fibrin-bound thrombin by a covalent antithrombin-heparin complex. *J. Biochem.* **132**, 167–176
7. Chan, A.K.C., Berry, L., Klement, P., Julian, J., Mitchell, L., Weitz, J., Hirsh, J., and Andrew, M. (1998) A novel antithrombin-heparin covalent complex: antithrombotic and bleeding studies in rabbits. *Blood Coagul. Fibrinolysis* **9**, 587–595
8. Chan, A.K.C., Rak, J., Berry, L., Liao, P., Vlasin, M., Weitz, J., and Klement, P. (2002) Antithrombin-heparin covalent complex: A possible alternative to heparin for arterial thrombosis prevention. *Circulation* **106**, 265
9. Berry, L., Chan, A.K.C., and Andrew, M. (1998) Polypeptide-polysaccharide conjugates produced by spontaneous non-enzymatic glycation. *J. Biochem.* **124**, 434–439
10. Paredes, N., Wang, A., Berry, L.R., Smith, L.J., Stafford, A.R., Weitz, J.I., and Chan, A.K.C. (2003) Mechanisms responsible for catalysis of the inhibition of factor Xa or thrombin by antithrombin using a covalent antithrombin-heparin complex. *J. Biol. Chem.* **278**, 23398–23409
11. Berry, L., Stafford, A., Fredenburgh, J., O'Brodovich, H., Mitchell, L., Weitz, J., Andrew, M., and Chan, A.K.C. (1998) Investigation of the anticoagulation mechanisms of a covalent antithrombin-heparin complex. *J. Biol. Chem.* **273**, 34730–34736
12. Brennan, S.O., George, P.M., and Jordan, R.E. (1987) Physiological variant of antithrombin-III lacks carbohydrate sidechain at Asn 135. *FEBS Lett.* **219**, 431–436
13. Chan, A.K.C., Berry, L.R., Paredes, N., and Parmar, N. (2003) Isoform composition of antithrombin in a covalent antithrombin-heparin complex. *Biochem. Biophys. Res. Commun.* **309**, 986–991
14. Carrell, R.W., Stein, P.E., Fermi, G., and Wardell, M.R. (1994) Biological implications of a 3 Å structure of dimeric antithrombin. *Structure* **2**, 257–270
15. Bjork, I., Ylinenjärvi, K., Olson, S.T., and Bock, P.E. (1992) Conversion of antithrombin from an inhibitor of thrombin to a substrate with reduced heparin affinity and enhanced conformational stability by binding of a tetradecapeptide corresponding to the P1 to P14 region of the putative reactive bond loop of the inhibitor. *J. Biol. Chem.* **267**, 1976–1982
16. Schechter, I. and Berger, A. (1967) On the size of the active site in proteases. I. Papain. *Biochem. Biophys. Res. Commun.* **27**, 157–162
17. Berger, A., Schechter, I., and Berger, A. (1967) On the size of the active site in proteases II. Carboxypeptidase-A. *Biochem. Biophys. Res. Commun.* **29**, 862–867
18. Schechter, I. and Berger, A. (1968) On the active site of proteases. III. Mapping the active site of papain; Specific peptide

inhibitors of papain. *Biochem. Biophys. Res. Commun.* **32**, 898–902
19. Islam, T., Butler, M., Sikkander, S.A., Toida, T., and Linhardt, R.J. (2002) Further evidence that periodate cleavage of heparin occurs primarily through the antithrombin binding site. *Carbohydr. Res.* **337**, 2239–2243
20. Manson, H.E., Austin, R.C., Fernandez-Rachubinski, R., Rachubinski, R.A., and Blajchman, M.A. (1989) The molecular pathology of inherited human antithrombin III deficiency. *Transfus. Med. Rev.* **3**, 264–291
21. Means, G.E. and Feeney, R.E. (1995) Reductive alkylation of proteins. *Anal. Biochem.* **224**, 1–16
22. Hatton, M.W.C., Berry, L.R., and Regoeczi, E. (1978) Inhibition of thrombin by antithrombin III in the presence of certain glycosaminoglycans found in the mammalian aorta. *Thromb. Res.* **13**, 655–670
23. Jones, T.A., Zou, J.-Y., and Cowen, S.W. (1991) Improved methods for building models in electron density maps and the location of errors in these models. *Acta Crystallogr. A* **47**, 110–119
24. Kleywegt, G.J. and Jones, T.A. (1997) Model-building and refinement practice. *Methods Enzymol.* **277**, 208–230
25. Lindahl, U., Thunberg, L., Bäckström, G., Riesenfeld, J., Nordling, K., and Björk, I. (1984) Extension and structural variability of the antithrombin-binding sequence in heparin. *J. Biol. Chem.* **259**, 12368–12376
26. Razi, N., Feyzi, E., Bjork, I., Naggi, A., Casu, B., and Lindahl, U. (1995) Structural and functional properties of heparin analogues obtained by chemical sulphation of *Escherichia coli* K5 capsular polysaccharide. *Biochem J.* **309**, 465–472
27. Stone, A.L., Beeler, D., Oosta, G., and Rosenberg, R.D. (1982) Circular dichroism spectroscopy of heparin-antithrombin interactions. *Biochemistry* **79**, 7190–7194
28. Owen, M.C., Beresford, C.H., and Carrell, R.W. (1988) Antithrombin Glasgow, 393 Arg to His: a P1 reactive site variant with increased heparin affinity but no thrombin inhibitory activity. *FEBS Lett.* **231**, 317–320
29. Mille, B., Watton, J., Barrowcliffe, T.W., Mani, J.-C., and Lane, D.A. (1994) Role of N- and C-terminal amino acids in antithrombin binding to pentasaccharide. *J. Biol. Chem.* **269**, 29435–29443
30. Chang, W.S.W., Wardell, M.R., Lomas, D.A., and Carrell, R.W. (1996) Probing serpin reactive-loop conformations by proteolytic cleavage. *Biochem J.* **314**, 647–653
31. Pike, R.N., Potempa, J., Skinner, R., Fitton, H.L., McGraw, W.T., Travis, J., Owen, M., Jin, L., and Carrell, R. (1997) Heparin-dependent modification of the reactive centre arginine of antithrombin and consequent increase in heparin binding Affinity. *J. Biol. Chem.* **272**, 19652–19655
32. Olson, S.T., Björk, I., Sheffer, R., Craig, P.A., Shore, J.D., and Choay, J. (1992) Role of the antithrombin-binding pentasaccharide in heparin acceleration of antithrombin-proteinase reactions: Resolution of the antithrombin conformational change contribution to heparin rate enhancement. *J. Biol. Chem.* **267**, 12528–12538